Magnetic-fluorescent nanocomposites for biomedical multitasking†

Serena A. Corr,[a] Aisling O' Byrne,[a] Yurii K. Gun'ko,*[a] Swapankumar Ghosh,[b] Dermot F. Brougham,[b] Siobhan Mitchell,[c] Yuri Volkov[c] and Adriele Prina-Mello[d]

Received (in Cambridge, UK) 27th July 2006, Accepted 7th September 2006
First published as an Advance Article on the web 29th September 2006
DOI: 10.1039/b610746j

Fluorescent magnetite nanocomposites based on magnetic nanoparticles, a polyhedral octaaminopropylsilsesquioxane and a porphyrin derivative have been prepared. The intracellular uptake of the nanocomposites by macrophage and bone osteoblast cells, and their potential as MRI contrast agents, has been demonstrated.

Magnetic nanomaterials are of immense importance in the emerging area of nanomedicine.[1] In particular, the use of magnetic nanoparticles, as diagnostic tools in MRI contrast agents,[2] as mediators for hyperthermic cancer treatment,[3] and as drug delivery vehicles,[4] are rapidly expanding fields. It has been suggested that, as the small size increases their blood circulation time, magnetic nanoparticles could be functionalised *via* conjugation to various monoclonal antibodies, peptides, or proteins to achieve their targeted localisation.[5] Some recent research has also focused on the preparation and biological applications of dye-containing fluorescent magnetic nanoparticles.[6,7]

Porphyrins are biocompatible fluorescent compounds which have been used as efficient photosensitisers for photodynamic therapy, a technique whereby tumour tissue is destroyed by the uptake of dye and subsequent irradiation with visible light.[8] Magnetic nanoparticles stabilised by fluorescent molecules, such as porphyrins, would offer great diagnostic and therapeutic possibilities and would have the potential to be positioned by an applied external magnetic field. However, the fabrication of useful composites presents several challenges, primarily because the magnetic cores normally quench the porphyrin fluorescence. This problem can be partially resolved by covalent bonding of porphyrin to magnetite nanoparticles *via* an appropriate spacer.[7]

In this work we describe the preparation of a new type of "two in one" fluorescent-magnetic nanocomposites based on magnetite nanoparticles, a polyhedral octaaminopropylsilsesquioxane ($T_8NH_3^+Cl^-$),[9] and a porphyrin derivative. We also assess their intracellular uptake and evaluate their potential as MRI contrast agents.

Magnetite nanoparticles were prepared by reacting a mixture of ferrous and ferric chlorides (2 : 1 molar ratio) and NaCl aqueous solution with ammonia.‡ A suspension of the particles in distilled Millipore water was prepared using ultrasound. The suspension was then treated with the octaaminopropylsilsesquioxane hydrochloride $T_8NH_3^+Cl^-$.†[9] Finally a solution of 4,4′,4″,4‴-(21H,23H-porphine-5,10,15,20-tetrayl) tetrakis-(benzoic acid) was added to the magnetite suspension. Any precipitate was removed by magnetic separation and further aggregates were removed by centrifugation giving a stable suspension of $T_8NH_3^+Cl^-$–porphyrin magnetite nanocomposites in water. These nanocomposites are formed *via* non-covalent ionic and hydrogen bonding interactions between the magnetic nanoparticle surface, $T_8NH_3^+$ ions and porphyrin molecules which contain terminal carboxylate groups. The interaction between polyamines and coproporphyrin tetranions has been previously investigated.[10]

TEM images of the magnetite–porphyrin nanocomposites have shown the formation of partially aggregated core–shell nanoparticles (Fig. 1). The particle size is found to be 12 $\pm$ 2 nm (N = 100 particles). By analysing the HRTEM images of a single functionalized magnetite nanoparticle, the lattice spacing between two planes is 4.82 Å, corresponding to the distance between two (111) planes in Fe_3O_4 (Fig. 1d).

IR spectra of the nanocomposites reveal the presence of both the $T_8NH_3^+Cl^-$ stabiliser and the porphyrin complex.† Powder X-ray diffraction patterns coincide with the JCPDS database for magnetite.†

Fluorescence spectra of $T_8NH_3^+Cl^-$–porphyrin–magnetite composite in phosphate buffer (3 mM, pH 7.2) have shown emission

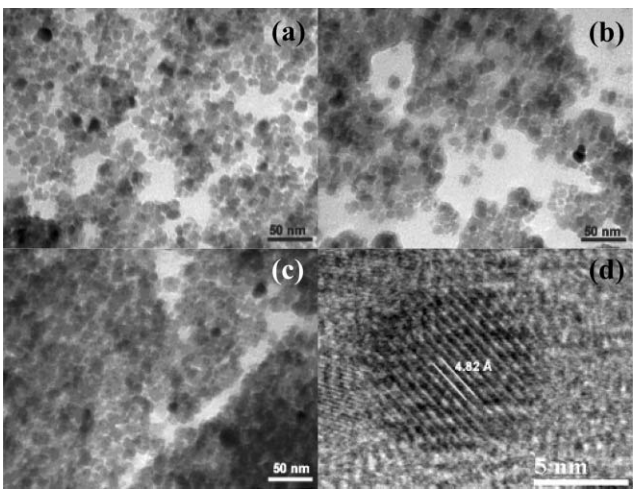

Fig. 1 TEM images of (a) Initial magnetite nanoparticles, after functionalisation with (b) $T_8NH_3^+Cl^-$; (c) after functionalisation with $T_8NH_3^+Cl^-$ and porphyrin, (d) HRTEM of $T_8NH_3^+Cl^-$porphyrin composite.

[a]*School of Chemistry, Trinity College Dublin, Dublin 2, Ireland. E-mail: igounko@tcd.ie; Fax: +353-1-671 2826; Tel: +353-1-608 3543*
[b]*National Institute for Cellular Biotechnology, School of Chemical Sciences, Dublin City University, Dublin 9, Ireland*
[c]*Department of Clinical Medicine, Trinity College Dublin, Dublin 2, Ireland*
[d]*Centre for Research on Adaptive Nanostructures and Nanodevices, Trinity College Dublin, Dublin 2, Ireland*

† Electronic supplementary information (ESI) available: Experimental details, spectra of nanocomposites, micrographs of cells with nanocomposites. See DOI: 10.1039/b610746j

peaks at 645 and 706 nm, with associated excitation peaks at 413, 518, 556 and 585 nm (Fig. 2). The strong fluorescent emission of the composites proves that the $T_8NH_3^+$ ions surrounding the core of the magnetite nanoparticle prevent the quenching of the luminescence of the connected porphyrin moieties.

The magnetic nature of the nanoparticle composites and their potential MRI contrast efficiency was assessed by nuclear magnetic resonance dispersion (NMRD), where the frequency dependence of the spin–lattice relaxation is measured. The water relaxation rate enhancement due to the superparamagnetic particles is expressed as concentration independent relaxivity, r_1 with units s^{-1} mM^{-1} (of Fe). The NMRD profiles measured for both the $T_8NH_3^+Cl^-$–magnetite and $T_8NH_3^+Cl^-$–porphyrin–magnetite are shown in Fig. 3. The relaxivity values obtained for these samples are slightly higher than those for commercial nanoparticulate MRI contrast agents at 20 MHz. TEM demonstrates that the particles are in the superparamagnetic size range,

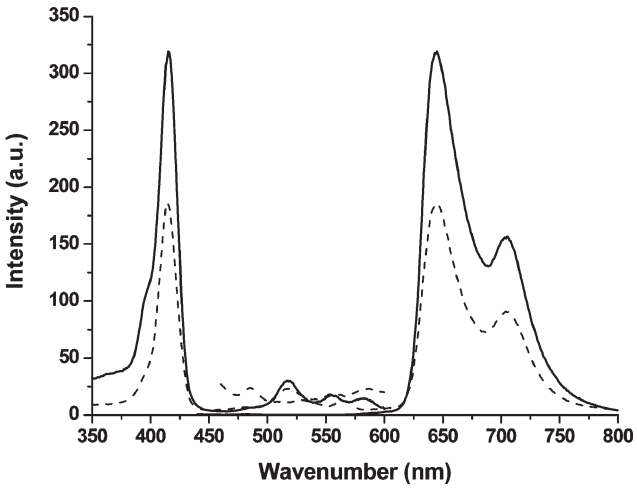

Fig. 2 Emission (right) and excitation (left) spectra of original porphyrin (1.4×10^{-9} M in phosphate buffer, solid line) and porphyrin–$T_8NH_3^+Cl^-$–magnetite nanocomposites (360 μL of particle suspension, made up to 3 mL with phosphate buffer, dashed line).

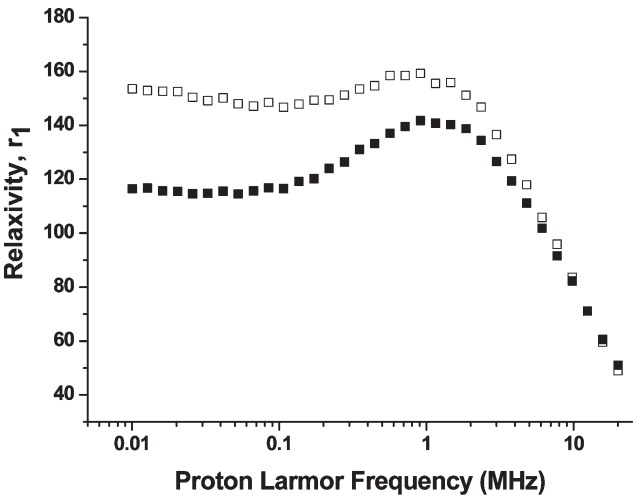

Fig. 3 NMRD response recorded at 25 ± 1 °C, of $T_8NH_3^+Cl^-$ magnetite (□) and porphyrin–$T_8NH_3^+Cl^-$ magnetite (■) nanocomposites.

and the observed r_1 maxima clearly indicate[11] that a significant proportion, *ca.* 60 mol%, of the magnetisation is superparamagnetic.[12] However, the high low-field relaxivity shows that the remaining magnetisation is magnetically blocked. This is most likely due to strong anisotropic interparticle interactions in the magnetic nanoclusters, which are more predominant for the $T_8NH_3^+Cl^-$–magnetite. PCS measurements confirm the presence of clusters in suspension, giving a Z-average cluster size of 82 nm with a PDI of 0.415.

We have investigated the uptake and cellular localisation of porphyrin–$T_8NH_3^+Cl^-$–magnetite nanocomposites in live THP-1 phagocytic cell line. THP-1 cells were differentiated to macrophages and the nanocomposites were added at a 1 in 100 dilution followed by incubation for the indicated times at 37 °C. Vigorous washing with PBS (Phosphate Buffer Saline) followed the incubation period to detach the loosely bound nanoparticles. Confocal imaging found that the porphyrin–$T_8NH_3^+Cl^-$–magnetite nanocomposites are internalized by the macrophages and sequestered to the cytoplasm within 10 min (Fig. 4), significantly increasing the fluorescent signal due to intracellular particle accumulation, compared to the non-ingested nanocomposites.

Further cell–nanoparticle interaction studies demonstrated that the hybrid ($T_8NH_3^+Cl^-$–porphyrin–magnetite) nanoparticles were also actively internalized by live osteoblast (MC3T3-E1) cells (ATCC, USA). Nanoparticles with an initial density of 10^{11} particles mL^{-1} were stabilised for 2 h in the cell culture medium (α-MEM, ATCC, USA), and added to adherent MC3T3-E1 cells at a final concentration of 10^6 particles mL^{-1} and incubated at 37 °C, 5% CO_2 and 95% RH for 30 min on a glass coverslip.

The confocal and phase contrast microscopy images shown in Fig. 5 are taken from different batches of MC3T3-E1 cells and are representative of the extent of magnetic particle internalisation by groups of cells (Fig. 5a,b) and of localisation of the particles in specific organelles within a cell (Fig. 5c,d). Control cell samples which had been exposed to porphyrin dye only, in the same concentration range, were imaged in parallel. For all of these samples, no internalisation of the porphyrin dye was observed.†

Diffuse staining inside the cytoplasm, observed by confocal fluorescence imaging, demonstrated that a significant fraction of the particles is internalized by the cells. The aggregated porphyrin nanocomposites are most likely taken up by the cells *via* endocytosis.[13] The nanocomposites also exhibit a distinctive subcellular distribution corresponding to the location of the

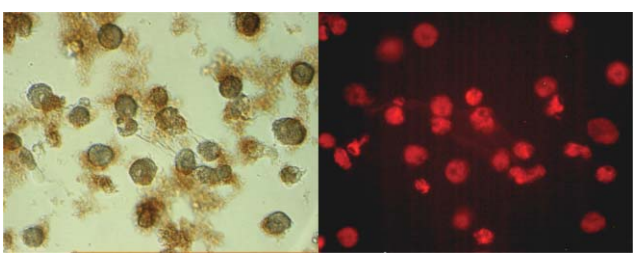

Fig. 4 Porphyrin–$T_8NH_3^+Cl^-$–magnetite nanocomposites in cultures of macrophages. Left, transmitted light microscopic image of the THP-1 cells interacting with nanocomposite particles. Right, corresponding fluorescent image of the same microscopic field (λ_{ex} = 488 nm, λ_{em} = 650 nm). Remaining non-ingested particles are seen as brown aggregates in transmitted light.

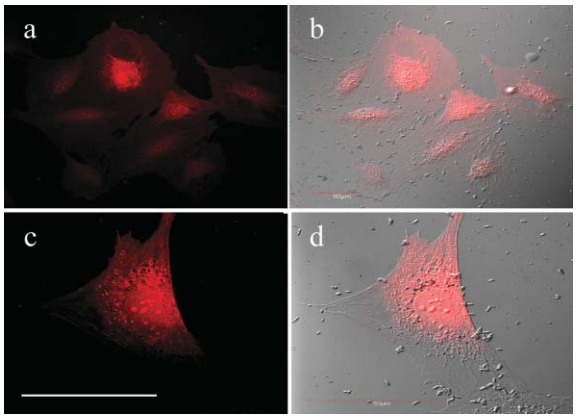

Fig. 5 Osteoblast cells uptake of particles. Population imaging (a) confocal image and (b) overlay with phase contrast (magnification ×40, scale bar = 50 μm). Single cell imaging (c) confocal image and (d) with combined phase contrast (magnification ×60, scale bar = 50 μm).

mitochondria, endoplasmic reticulum and nuclei. This phenomenon, as well as an unusually strong increase of the fluorescence inside the cells after particle uptake, might be related to dissociation of the components in the magnetic–fluorescent nanocomposites. We believe that porphyrin species released from the composites in this case are no longer exposed to the partial quenching effects by paramagnetic oxide cores. This opens up several intriguing possibilities. Firstly, the reduction of the overall size of the composites might enable better penetration of porphyrin molecules into size restricted intracellular compartments. Secondly, such intracellular fragmentation of the nanocomposites could potentially serve as a basis both for new subcellular imaging contrast agents and for targeted drug release systems.

Thus we have prepared new fluorescent porphyrin–$T_8NH_3^+Cl$–magnetite nanocomposites. The nanoparticles aggregate into larger magnetic clusters with strong anisotropic interparticle interactions that increase the low-field relaxivity. These magnetic suspensions are potential organelle specific diagnostic markers which could be detected by MRI or fluorescent confocal imaging. The results of our studies also indicate that these nanocomposites could potentially serve as drug delivery systems. We believe that these systems may have important applications in diagnostics and the treatment of degenerative and chronic diseases associated with overactive phagocytic responses, such as autoimmune disorders and osteoporosis. Future work will involve more detailed studies of the nature of the nanocomposites and the intracellular mechanisms of their interaction with live cells.

The authors thank the Trinity Centre for Bioengineering for the cell cultures, the Institute of Neuroscience for the confocal imaging facilities and the Centre for Microscopy and Analysis for use of TEM. We also thank Enterprise Ireland and CRANN-Science Foundation Ireland for financial support.

Notes and references

‡ Magnetite nanoparticles were prepared *via* well documented previously published procedures.[14] A mixture of ferrous and ferric chlorides (2 : 1 molar ratio; 4×10^{-2} mol dm^{-3} and 2×10^{-2} mol dm^{-3} respectively) and 100 mL of 1 M NaCl aqueous solution were treated with ammonia in a degassed aqueous solution at room temperature. The dark precipitate was washed with deoxygenated Millipore water (3 × 20 mL). A suspension of the particles (0.11 g) in Millipore water (20 mL) was prepared by placing the suspension in ultrasound for 30 min.

Octaaminopropylsilsesquioxane hydrochloride (see supporting information for preparation†) (0.2 g, 0.17 mmol) was dissolved in Millipore water (10 mL) and added to the magnetic suspension. The mixture was shaken overnight to give a stable suspension. Magnetic fluid (10 mL; as synthesised above) was placed in a sample tube. 4,4′,4″,4‴-(21H,23H-porphine-5,10,15,20-tetrayl) tetrakis-(benzoic acid) (1×10^{-2} g, 1.26×10^{-5} mol) was dissolved in 10 mL methanol. 50 μL of this solution was added to 10 mL of the magnetite suspension. The mixture was stirred at room temperature for 1 h. A sample was dried for IR analysis and XRD. NMRD analysis, UV-vis and fluorescence spectroscopy was carried out on the stable suspension.

1 (*a*) Q. A. Pankhurst, J. Connolly, S. K. Jones and J. Dobson, *J. Phys. D: Appl. Phys.*, 2003, **36**, R167–R181; (*b*) C. Bergemann, D. Müller-Schulte, J. Oster, L. à Brassard and A. S. Lübbe, *J. Magn. Magn. Mater.*, 1999, **194**, 45–52.
2 (*a*) R. N. Muller, A. Roch, J.-M. Colet, A. Ouakssim and P. Gillis, *The Chemistry of Contrast Agents in Medical Magnetic Resonance Imaging*, ed. A. E. Merbach and E. Toth, John Wiley and Sons Publishers, 2001, p. 417; (*b*) D. K. Kim, Y. Zhang, J. Kehr, T. Klason, B. Bjelke and M. Muhammed, *J. Magn. Magn. Mater.*, 2001, **225**, 256–261.
3 (*a*) A. Jordan, R. Scholz, P. Wust, H. Fähling and R. Felix, *J. Magn. Magn. Mater.*, 1999, **201**, 413–419; (*b*) A. Jordan, R. Scholz, K. Maier-Hauff, M. Johannsen, P. Wust, J. Nadobny, H. Schirra, H. Schmidt, S. Deger, S. Loening, W. Lanksch and R. Felix, *J. Magn. Magn. Mater.*, 2001, **225**, 118–126.
4 A. Senyei, K. Wider and C. Czerlinski, *J. Appl. Phys.*, 1978, **49**, 3578–3583.
5 L. G. Remsen, C. I. McCormick, S. Roman-Goldstein, G. Nilaver, R. Weissleder, A. Bogdanov, K. E. Hellström, I. Hellström, R. A. Kroll and E. A. Neuwelt, *Am. J. Neuroradiol.*, 1996, **17**, 411–418.
6 (*a*) M. Mikhaylova, D. K. Kim, C. C. Berry, A. Zagorodni, M. Toprak, A. S. G. Curtis and M. Muhammed, *Chem. Mater.*, 2004, **16**, 2344–2354; (*b*) L. Levy, Y. Sahoo, K.-S. Kim, E. J. Bergey and P. N. Prasad, *Chem. Mater.*, 2002, **14**, 3715–3721; (*c*) H. Lu, G. Yi, S. Zhao, D. Chen, L. H. Guo and J. Cheng, *J. Mater. Chem.*, 2004, **14**, 1336–1341; (*d*) F. Bertorelle, C. Wilhelm, J. Roger, F. Gazeau, C. Menager and V. Cabuil, *Langmuir*, 2006, **22**, 5385–5391.
7 H. Gu, K. Xu, Z. Yang, C. K. Chang and B. Xu, *Chem. Commun.*, 2005, **34**, 4270–4272.
8 (*a*) R. Bonnett, *Chem. Soc. Rev.*, 1995, **1**, 19; (*b*) I. Cecic and M. Korbelik, *Cancer Lett.*, 2002, **183**, 43–51.
9 F. J. Feher, K. D. Wyndham, D. Soulivong and F. Nguyen, *J. Chem. Soc., Dalton Trans.*, 1999, **9**, 1491–1497.
10 A. Flores-Villalobos, H. Morales-Rojas, A. Escalante-Tovar and A. K. Yatsimirsky, *J. Phys. Org. Chem.*, 2002, **15**, 83–93.
11 A. Roch, R. N. Muller and P. Gillis, *J. Chem. Phys.*, 1999, **110**, 5403–5411.
12 S. J. Byrne, S. A. Corr, Y. K. Gun'ko, J. M. Kelly, D. F. Brougham and S. Ghosh, *Chem. Commun.*, 2004, **22**, 2560–2561.
13 J. Osterloh and M. G. H. Vincente, *J. Porphyrins Phthalocyanines*, 2002, **6**, 305–324.
14 (*a*) X. P. Qiu, *Chin. J. Chem.*, 2000, **18**, 834–837; (*b*) R. Massart, *IEEE Trans. Magn.*, 1981, **17**, 1247–1248.

